

# Experimental Findings on Seismic Performance of a Point-Fixed Glass Façade System

**Eliana Inca-Cabrera <sup>a</sup>, Sandra Jordão <sup>a</sup>, Carlos Rebelo <sup>a</sup>, Chiara Bedon <sup>b</sup>, Afonso Mesquita <sup>c</sup>, Seyed-Amin Hosseini <sup>a</sup>**

- a University of Coimbra, ISISE, ARISE, Department of Civil Engineering, Portugal  
[e.inca.cabrera@uc.pt](mailto:e.inca.cabrera@uc.pt), [sjordao@dec.uc.pt](mailto:sjordao@dec.uc.pt), [crebelo@dec.uc.pt](mailto:crebelo@dec.uc.pt), [S.AMIN9068@gmail.com](mailto:S.AMIN9068@gmail.com)
- b University of Trieste, UNITS, Department of Engineering and Architecture, Italy,  
[chiara.bedon@dia.units.it](mailto:chiara.bedon@dia.units.it)
- c Polytechnic Institute of Castelo Branco IPCB, Higher School of Technology, Castelo Branco, Portugal,  
[mesquita.acb@gmail.com](mailto:mesquita.acb@gmail.com)

## Abstract

This paper presents the outcomes of a full-scale experimental and numerical investigation on the in-plane cyclic response of point-fixed glass façade systems (PFGFS). Two façade prototypes with different connector types—fully drilled countersunk bolts and partially embedded bolts—were tested under quasi-static reversed loading to evaluate their drift capacity and post-fracture performance. The 3×3 panel configurations exhibited stable cyclic behaviour with maximum drift ratios near 2%, exceeding current code limits for non-structural ductile elements. Damage progression was governed by bolt rotation, sealant deformation, and limited yielding of steel components, while the laminated glass and interlayer ensured post-fracture stability without panel fallout. A simplified finite element model, validated against test data, accurately captured the global stiffness and deformation trends. The results demonstrate that PFGFS can sustain controlled failure mechanisms while maintaining residual load-bearing capacity, supporting the development of performance-based seismic design criteria for glass façades.

## Keywords

Point-fixed glass façade; In-plane drift; Seismic performance; Laminated glass; Finite element modelling

## Article Information

- Digital Object Identifier (DOI): [10.47982/cgc.10.726](https://doi.org/10.47982/cgc.10.726)
- Published by [Challenging Glass](#), on behalf of the author(s), at [Stichting OpenAccess](#).
- Published as part of the peer-reviewed [Challenging Glass Conference Proceedings](#), Volume 10, June 2026, [10.47982/cgc.10](https://doi.org/10.47982/cgc.10)
- Editors: Christian Louter, Freek Bos & Jan Belis
- This work is licensed under a [Creative Commons Attribution 4.0 International](#) (CC BY 4.0) license.
- Copyright © 2026 with the author(s)

## 1. Introduction

The growing use of glass in façade systems has introduced new challenges for seismic design. Point-fixed glass façade systems (PFGFS) are gradually more adopted due to their high level of transparency and architectural expression (Fig. 1a); however, they are particularly vulnerable to in-plane deformation demands arising from seismic actions or wind-induced racking. Observations from past earthquakes have highlighted significant damage to non-structural glass components (Fig. 1b), underscoring the need for improved performance-based design criteria for glass façades (Taghavi and Miranda 2003).

Existing research has primarily focused on framed glazing systems (Behr 1998; Sivanerupan et al. 2014; AAMA 501.4 2001), whereas the in-plane cyclic behaviour of PFGFS remains comparatively underexplored. Current drift limits used in practice are largely derived from frame-supported systems and have been shown to be inadequate for capturing the distinct structural behaviour of point-fixed façades (Inca et al. 2019). The present study aims to quantify the in-plane drift capacity and damage progression of full-scale PFGFS subjected to cyclic loading and to identify the key mechanisms governing energy dissipation and post-fracture integrity. The outcomes contribute to a better understanding of the seismic response of point-fixed glass façades and support the development of performance-based design approaches tailored to their specific structural characteristics.



a) Front entry of Lisbon Airport.



b) PFGF failure (Perrone et al. 2019).

Fig. 1: Examples of PFGFS and current research experimental tests.

## 2. Experimental Campaign

### 2.1. Test layout and specimens

The experimental programme was designed to investigate the in-plane cyclic response of a point-fixed laminated glass façade system (PFGFS). Two full-scale façade mock-ups were tested under quasi-static cyclic loading (Inca et al. 2025) at the Laboratory of Structures, Construction and Structural Mechanics, Department of Civil Engineering, University of Coimbra, in collaboration with the ISISE research centre. The study was carried out within the framework of the GF-Seismic research project (Structural glass façades subjected to seismic loading, FCT POCI-01-0145-FEDER-032539) (Inca 2025).

Each test layout comprised nine laminated glass panels measuring  $1490 \times 1490$  mm, arranged in a  $3 \times 3$  grid and supported by a steel substructure (Fig. 2). The supporting system consisted of a S355 steel frame formed by four circular hollow section (CHS) columns ( $139.7 \times 8$  mm), connected at the top by

a rectangular hollow section (RHS) beam (200 × 120 × 12 mm) (Fig. 3). The columns were hinged at both ends, while out-of-plane displacements were restrained at the same locations to reproduce façade boundary conditions.

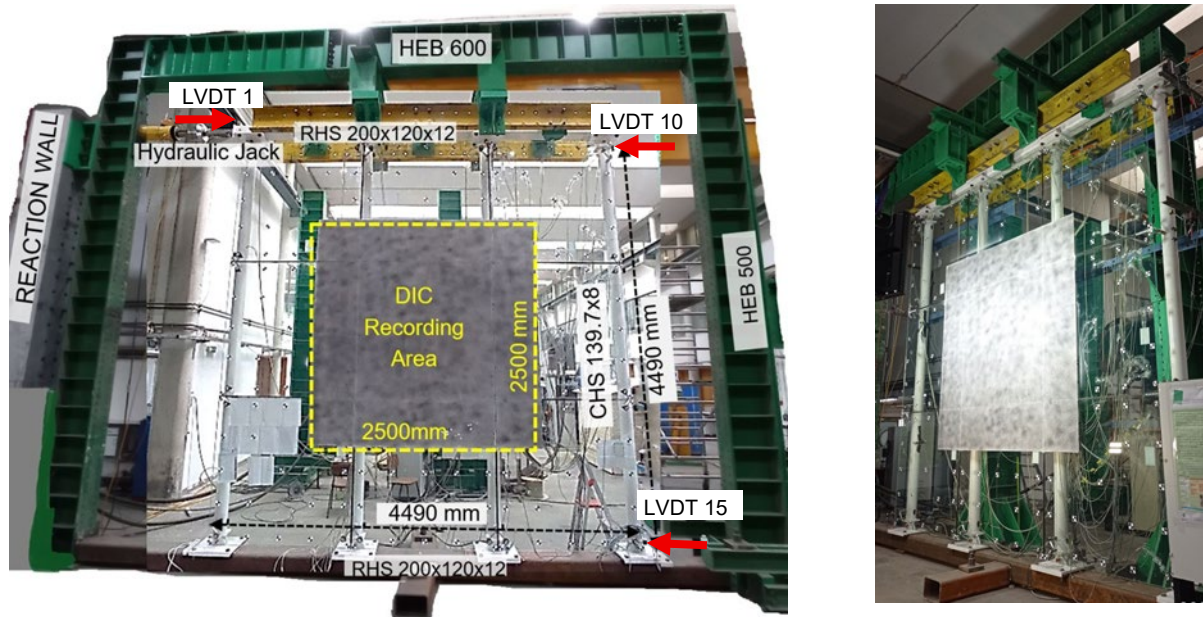


Fig. 2: Layout overview.

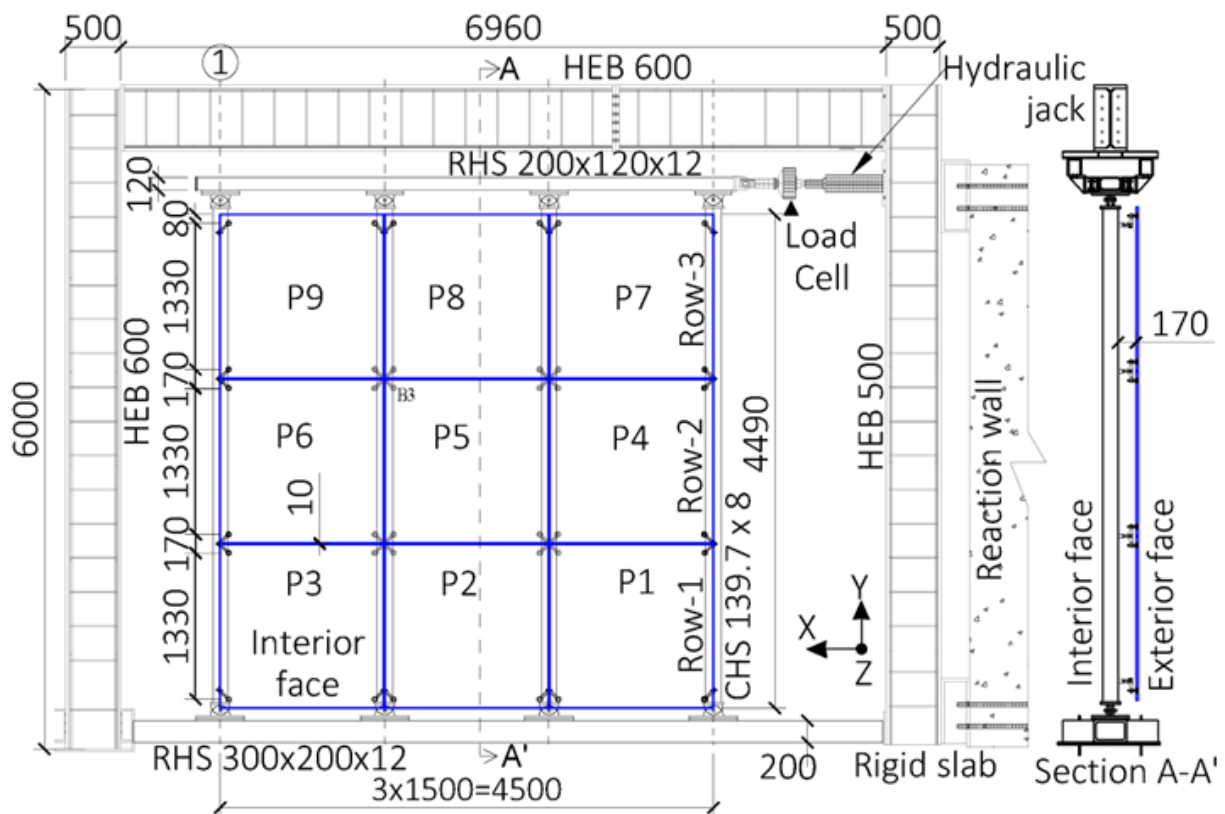


Fig. 3: General layout for the point-fixed glass façade cyclic tests (dimensions in mm).

Two connection configurations were investigated:

1. Fully drilled bolts (Test 1) – conventional through-bolts with countersunk heads.
2. Partially embedded bolts (Test 2) – semi-adhesive connectors with the bolt head embedded within the inner glass ply.

The glass panels consisted of 17.52 mm laminated fully tempered glass (6 mm + 10 mm plies) bonded with a 1.52 mm EVASAFE® interlayer (Fig. 4). The joints between adjacent panels were sealed using 10 mm of structural silicone (Sika® 2025), providing a secondary load-transfer mechanism.

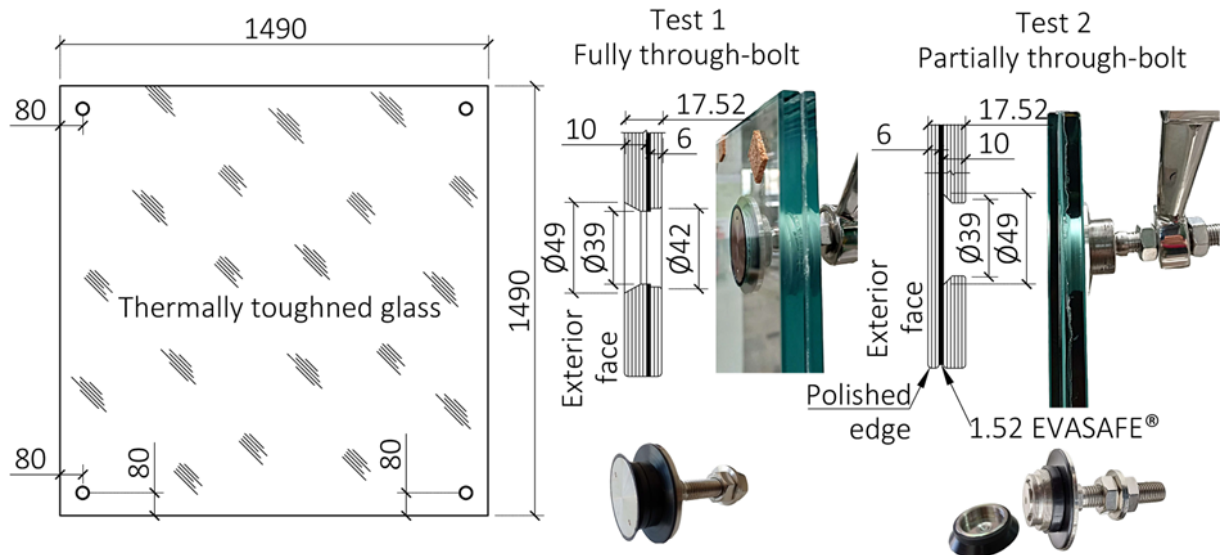


Fig. 4: Layout and geometry of the glass panels and fixings (dimensions in mm).

Prior to testing, the specimens were stored under controlled laboratory conditions at a mean temperature of 18 °C and an average relative humidity of 60%. During the experimental programme, the laboratory temperature remained stable, varying between 18.3 °C and 20.1 °C, as monitored at five control points. No measurable influence of temperature variations on the mechanical response of the laminated glass panels was observed. The mechanical properties of the materials employed in the experimental campaign are summarised in Table 1.

Table 1: Material mechanical properties.

Property	EVASAFE	Stainless Steel	Steel S355	Glass	Silicone
Specific weight, $\gamma$ [kN/m <sup>3</sup> ]	9.5	78.5	77.0	25.0	14.7
Young modulus, E [GPa]	12	202	203	70.0	3E-4
Poisson's ratio, $\nu$ [m/m]	0.53	0.30	0.30	0.21	-
Yielding stress, $\sigma_y$ [MPa]	-	208	430	-	-
Ultimate stress, $\sigma_u$ [MPa]	20.8	750	627	-	1
Ultimate strain, $\epsilon_u$ [%]	350.0	36.7	14.7	-	800.0

## 2.2. Test setup and loading protocol

In-plane lateral loading was applied using a hydraulic actuator anchored to a reaction wall. The displacement history followed the FEMA 461 (2007) quasi-static cyclic protocol, with progressively increasing displacement amplitudes applied under displacement control until glass fracture occurred (Fig. 5). Out-of-plane movement of the façade was restrained throughout the tests. The instrumentation system included linear variable displacement transducers (LVDTs), strain gauges, and optical measurement techniques to monitor global and local deformations. Photogrammetry was employed near the panel edges to capture in-plane displacements in the x–y plane, while digital image correlation (DIC) was used at the centre of the façade over an area of approximately 2.5 m × 2.5 m, enabling full-field displacement measurements in three directions.

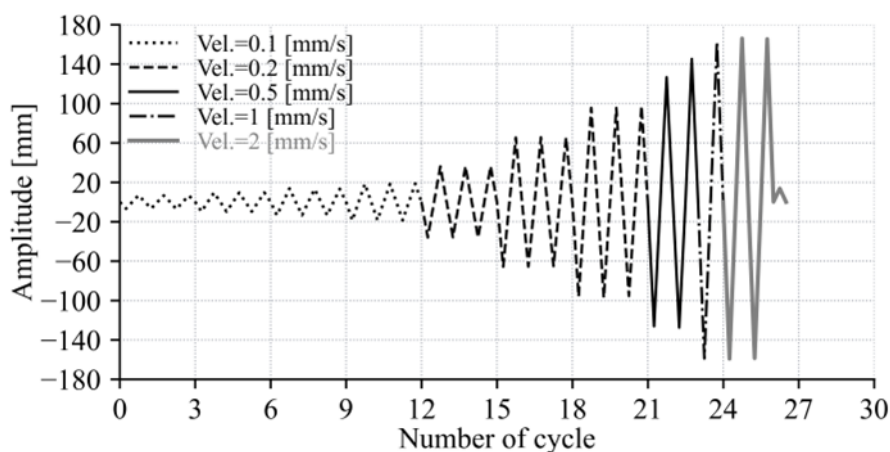


Fig. 5: Load protocol for cyclic tests.

## 3. Experimental results

Both façade configurations exhibited comparable global responses under in-plane cyclic loading. The in-plane drift ratio (DR) was calculated as the ratio between the relative displacement measured by LVDTs 10 and 15 and the distance separating these measurement points (4330 mm). Initial visible cracking was observed at drift ratios of approximately 2%, typically occurring in panels located at mid-height. Despite local glass fracture, both systems remained stable and were able to sustain additional loading cycles. The laminated interlayer effectively retained fractured glass fragments, preventing panel fallout, while the structural silicone joints accommodated deformations of up to 50% of their original thickness without loss of integrity. The load–displacement responses showed stable hysteretic behaviour, with slight asymmetry attributed to friction and residual locking effects at the connections. Maximum in-plane drift ratios of 2.12% and 2.28% were recorded for Test 1 (Fig. 6a) and Test 2 (Fig. 6b), respectively. Energy dissipation was primarily governed by bolt rotation and local yielding, enabling ductile behaviour and preventing brittle collapse.

The cyclic response can be divided into four distinct behavioural regimes showing specific manifestations of progressive damage, consistently observed in both tests (Fig. 6 and Table 2). These phases are summarized in:

1. Phase 1: Elastic behaviour with no visible damage (in-plane drift ratio < 0.8%)
2. Phase 2: Minor sealant softening and bolt rotation (in-plane drift ratio ~1%)
3. Phase 3: Pronounced shear at joints and washer deformation (in-plane drift ratio 1.3–1.8%)
4. Phase 4: Glass fracture in mid-row panels (in-plane drift ratio ~2%)

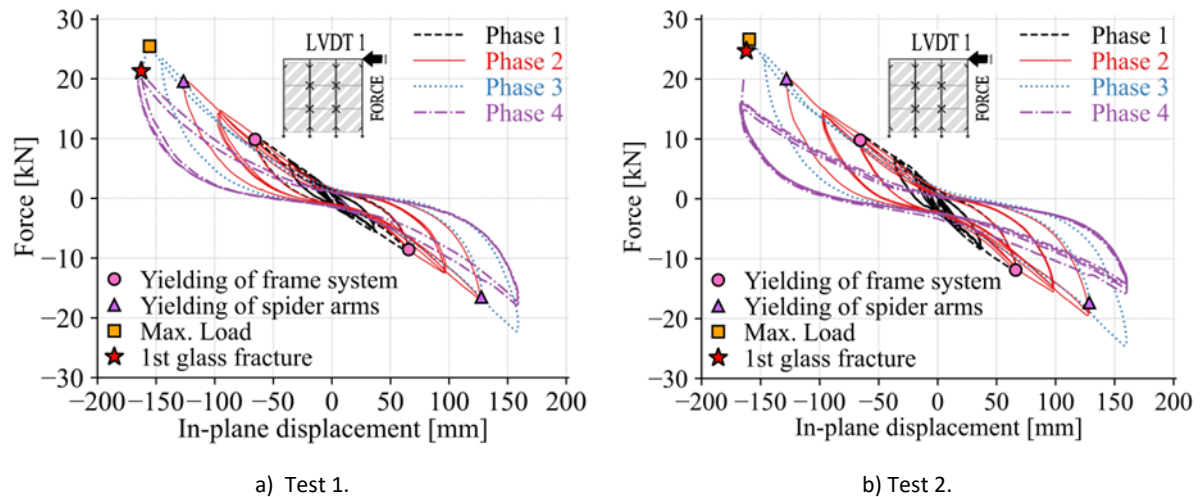


Fig. 6: Experimental results for lateral load versus in-plane displacement at the top beam of the glass façade frame, with main response events indicated.

Table 2: Progressive damage stages in PFLGF tests versus in-plane drift ratios.

Test 1		Test 2		Description of progressive damage
DR	MLD	DR	MLD	
[%]	[mm]	[%]	[mm]	
0.80	25.73	0.80	27.38	No visible damage
1.00	48.28	1.00	49.18	Paint peeling / Small damage in sealant
1.30	72.54	1.30	74.54	Shear at joints + rotation of bolts
1.80	95.62	1.80	101.58	High shear in joints + rotation of bolts + High out-of-plane displacement.
2.10	120.57	1.95	109.98	Collapse of one panel / Drop of load
2.28	121.16	1.99	111.00	Maximum drift after collapse

DR – Drift ratio | MLD – Maximum lateral displacement at LVDT 10

The first phase, corresponding to the elastic response of the system (Fig. 7a), was characterised by nearly coincident ascending and descending branches of the load–displacement curves, indicating a fully reversible behaviour with no permanent damage. In this regime, the imposed lateral deformation was mainly accommodated through the rotational capacity of the hinged connectors (approximately 7°), which allowed a combined vertical and horizontal movement of the panels. This mechanism was further supported by the shear deformability of the structural silicone joints, enabling relative panel

displacements without significant stress accumulation. This elastic phase extended up to drift levels close to 1%, with negligible residual deformation observed upon unloading.

When this threshold was exceeded, the system entered a second regime, marked by the onset of yielding within the steel support frame. This transition was evidenced by a clear separation between the loading and unloading branches of the hysteretic response. The progressively increasing area enclosed by successive load cycles confirmed the activation of energy dissipation mechanisms. In this phase, the steel frame contributed significantly to the global response, playing a dominant role in enhancing the overall ductility of the façade under reversed cyclic loading. As illustrated in Fig. 7b, elevated shear forces developed in the vicinity of the spider connectors, particularly in panels located at mid-height. Concurrently, noticeable out-of-plane displacements were recorded at the panel edges, revealing the development of bidirectional shear interaction within the silicone joints (Fig. 7c).

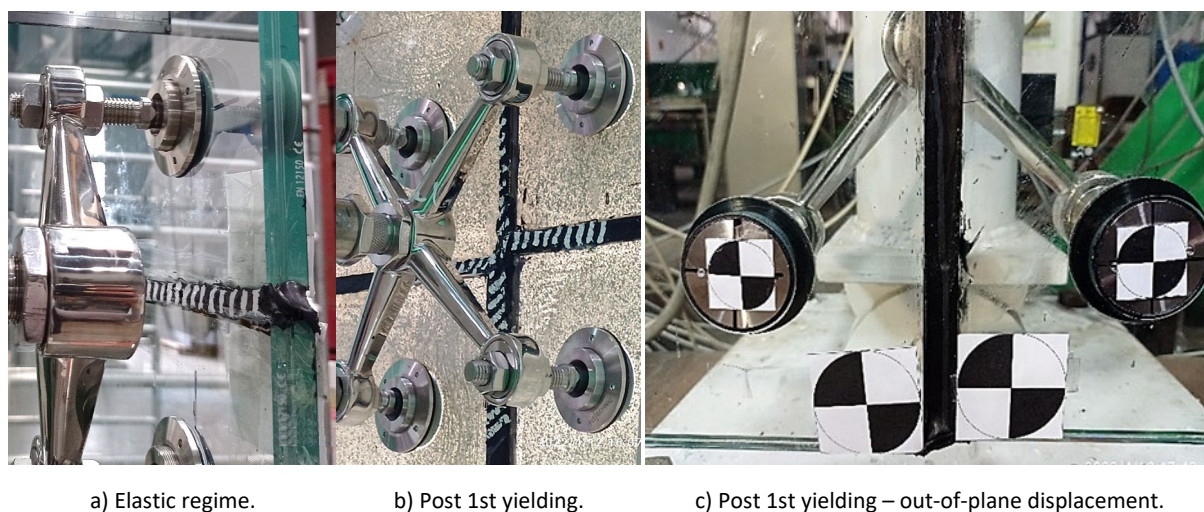
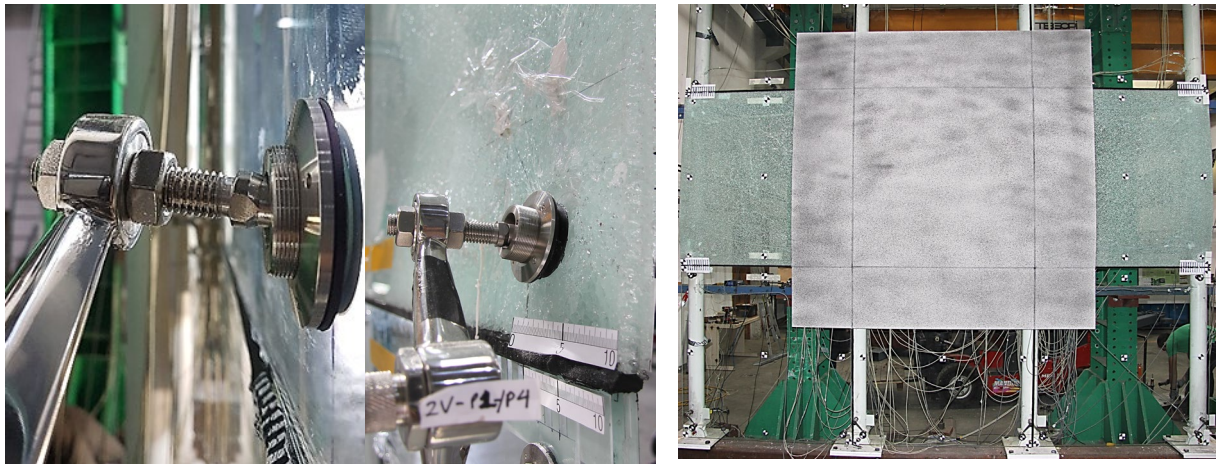


Fig. 7: Progressive damage in façade at early stages.

The third regime was activated at higher drift levels and was associated with the yielding of stainless-steel spider elements. At this stage, several connectors reached their maximum rotational capacity and transitioned from free rotation to partial bearing contact (Fig. 8a). This change in load-transfer mechanism, combined with pre-existing micro-defects near the bolt holes, led to a progressive intensification of local stress concentrations in the glass. With increasing cyclic demand, these effects caused a gradual degradation of the glass strength, ultimately resulting in the fracture of one or more panels (Fig. 8b). The pronounced reduction in global stiffness observed after fracture was primarily associated with the loss of the panels' in-plane diaphragm action: once both glass plies fractured, the fully tempered glass disintegrated into small fragments, effectively eliminating any residual bending resistance.

Despite the occurrence of glass fracture, the façade system remained globally stable and capable of sustaining load. The presence of the laminated interlayer, together with the countersunk conical bolt heads, ensured effective retention of fractured glass and prevented panel fallout, thereby maintaining structural integrity (Fig. 8c). This residual load-bearing capacity highlights the robustness of the connection detailing and underscores the critical role of lamination and controlled mechanical restraint in ensuring the post-fracture safety and resilience of point-fixed glass façade systems.



a) Post 1st yielding of connectors.      b) Post glass failure.      c) Residual capacity after test – test 2.

Fig. 8: Progressive damage in façade at phases 3 and 4.

#### 4. Numerical Validation

A simplified finite element model was developed using SAP2000 (2020) to reproduce the experimental response of the tested façade systems. The steel substructure was modelled using beam elements, while the glass panels were represented as equivalent monolithic shell elements (Fig. 9a). The flexibility of the point-fixing connections was introduced through non-linear rotational springs, whose properties were calibrated based on the experimental results. The imposed displacement history was applied at the top joint of the steel beam, consistently with the experimental loading configuration. The simulated force–displacement response showed good agreement with the experimental results up to the onset of glass fracture, confirming the suitability of the simplified modelling strategy for pre-design and global performance assessment (Fig. 9b). The model was able to capture both the progressive stiffness degradation and the ultimate drift capacity, which approached 2%, in line with the experimental observations.

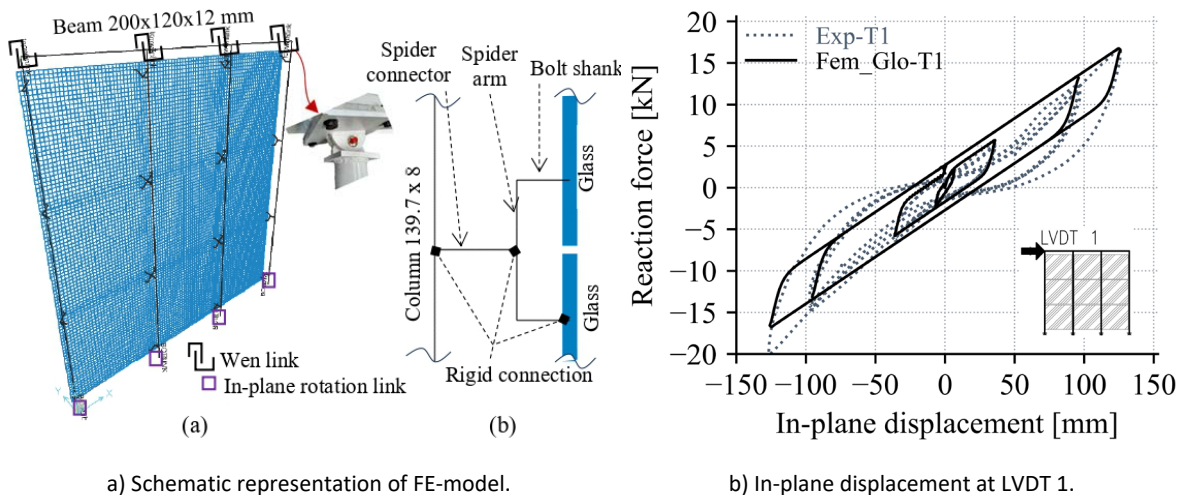


Fig. 9: Comparison between experimental and numerical results for test T-FTB.

Comparison with current seismic design standards, namely EN 1998 (2010) and FEMA 450 (2003), indicates that point-fixed laminated glass façade systems are capable of sustaining in-plane drift demands exceeding the typical ductility limits prescribed for non-structural elements, commonly in the range of 1.25–1.88%. However, these standards do not explicitly address the deformation mechanisms, connection behaviour, or post-fracture performance inherent to point-fixed laminated façades. As a result, their direct application to such systems introduces a degree of uncertainty in design. The results suggest that future design provisions would benefit from explicitly accounting for connection-specific rotational capacity, the layered composite behaviour of laminated glass, and the ability of these systems to maintain stability beyond first fracture. Such refinements would enhance safety, improve damage predictability, and strengthen the resilience of glazing systems under seismic loading.

The findings highlight the importance of allowing controlled rotation at bolted connections, using laminated glass with high-performance interlayers to ensure post-fracture integrity, and adopting flexible silicone joints to accommodate in-plane displacements. The introduction of performance-based drift limits specifically tailored to point-fixed façade systems—distinguishing between serviceability, damage, and ultimate limit states—would provide a more rational and reliable basis for design.

## 5. Conclusions

This paper presents the results of a full-scale experimental investigation carried out at the University of Coimbra on point-fixed laminated glass façade systems subjected to in-plane quasi-static cyclic loading. Two façade configurations, each comprising nine laminated glass panels arranged in a 3 × 3 grid, were tested to evaluate their drift capacity and post-fracture performance. The study examined two bolt-fixing solutions—fully drilled countersunk bolts and partially embedded bolts—to assess the influence of connection detailing on the global response. Both test configurations exhibited a progressive and controlled failure mechanism, with initial glass fracture consistently occurring in panels located in the middle row. Based on the experimental and numerical results, the following conclusions can be drawn:

- Both façade systems sustained in-plane drift ratios of approximately 2% prior to glass fracture, exceeding the drift limits commonly prescribed for non-structural elements in current seismic design standards.
- The global response was governed by progressive shear deformation and bolt rotation, rather than by brittle glass failure.
- Post-fracture stability was ensured by the laminated glass configuration and the use of countersunk conical bolt heads, preventing panel fallout
- The EVA type interlayer provided effective fragment retention and contributed to residual stiffness after fracture.
- The simplified finite element model successfully reproduced the main response features and proved suitable for design-stage assessment of similar façade systems.
- Findings encourage development of performance-based seismic design for glass façades.

## Acknowledgements

This work was partly financed by FCT / MCTES through national funds (PIDDAC) under the R&D Unit Institute for Sustainability and Innovation in Structural Engineering (ISISE), under reference UIDB / 04029/2020 ([doi.org/10.54499/UIDB/04029/2020](https://doi.org/10.54499/UIDB/04029/2020)), and under the Associate Laboratory Advanced Production and Intelligent Systems ARISE under reference LA/P/0112/2020

## References

- AAMA 501.4: recommended static test method for evaluating window wall, curtain wall and storefront systems subjected to seismic and wind-induced inter-story drift. Am. Archit. Manuf. Assoc. (2001)
- Behr, R.A.: Seismic performance of architectural glass in mid-rise curtain walls. *J. Archit. Eng.* 4(3), 94–98 (1998)
- FEMA 450: Recommended provisions for seismic regulations for new buildings and other structures. Fed. Emerg. Manag. Agency (2003)
- FEMA 461: Interim testing protocols for determining the seismic performance characteristics of structural and non-structural components. Fed. Emerg. Manag. Agency, Appl. Technol. Council. (2007)
- Inca, E., Jordão, S., Rebelo, C., Rigueiro, C., Simões, R.: Seismic behaviour of point-fixed glass façade systems: State-of-the-art review. *Eur. J. Eng. Sci. Technol.* 2(2), 1–15 (2019). <https://doi.org/10.33422/EJEST.2019.07.06>
- Inca-Cabrera, E.: Seismic behaviour of point-fixed glass façade systems. PhD Thesis, Univ. Coimbra (2025)
- Inca-Cabrera, E., Jordão, S., Rebelo, C., Bedon, C., Mesquita, A., Hosseini, S.A.: Experimental and numerical investigation of in-plane cyclic response of a point-fixed glass façade system for seismic performance assessment. *J. Build. Eng.* 96, 112956 (2025). <https://doi.org/10.1016/j.jobbe.2025.112956>
- NP EN 1998-1-1: Eurocode 8 — Design of structures for earthquake resistance — Part 1: General rules, seismic actions and rules for buildings. Eur. Comm. Stand. (2010)
- Perrone, D., Calvi, P.M., Nascimbene, R., Fischer, E.C., Magliulo, G.: Seismic performance of non-structural elements during the 2016 Central Italy earthquake. *Bull. Earthq. Eng.* 17(10), 5655–5677 (2019). <https://doi.org/10.1007/s10518-018-0361-5>
- SAP2000: Integrated software for structural analysis and design, Release 22. Comput. Struct., USA (2020)
- Sika Group: Sikasil® WS-605 S — High performance sealant: Data sheet (2025). <https://www.sika.com>. Accessed Dec 2025
- Sivanerupan, S., Wilson, J., Gad, E., Lam, N.: Drift performance of point-fixed glass façade systems. *Adv. Struct. Eng.* 17(10), 1491–1495 (2014). <https://doi.org/10.1260/1369-4332.17.10.1>
- Taghavi, S., Miranda, E.: Response assessment of non-structural building elements. PEER Rep. 2003/05, Pac. Earthq. Eng. Res. Cent. (2003)

## Platinum Sponsor

---



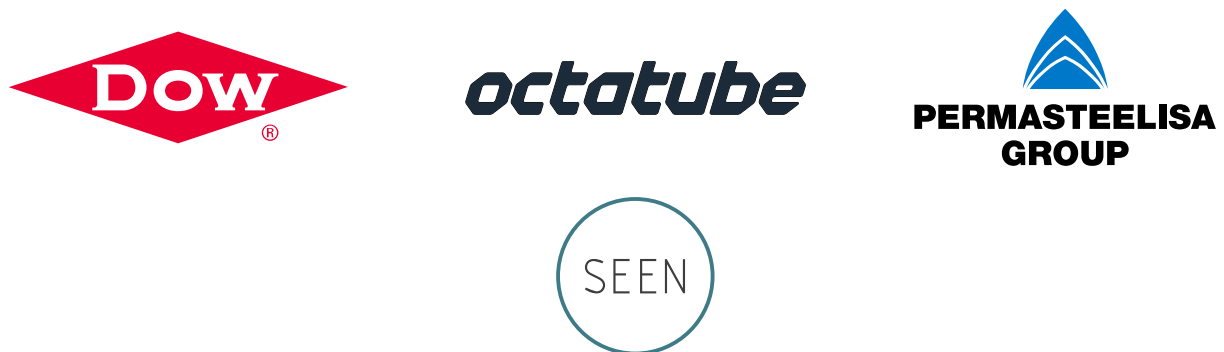
## Gold Sponsors

---



## Silver Sponsors

---



## Organisation

---

